Strain Monitoring By FBG Strain Sensor In a Small Scale Dam Model

Liang Ren, Jianyun Chen and Hong-Nan Li
School of Civil and Hydraulic Engineering, Dalian University of Technology, Liaoning, China

SUMMARY:
Accurate measurement of strain variation and effective prediction of failure within models has been a major objective for strain sensors in dam model tests. In this paper, a FBG strain sensor with enhanced strain sensitivity and packaged by two gripper tubes is presented and applied in the seismic tests of a small scale dam model. This paper discusses the principle of enhanced sensitivity of the FBG strain sensor. Calibration experiments and reliability tests were conducted to evaluate the sensor's strain transferring characteristics on plates of different material. This paper also investigates the applicability of the FBG strain sensors in seismic tests of a dam model by conducting a comparison between the test measurements of FBG sensors and analytical predictions, monitoring the failure progress and predicting the cracking inside the dam model. Results of the dam model tests prove that this FBG strain sensor has the advantages of small size, high precision and embedability, demonstrate promising potential in cracking and failure monitoring and in identification of the dam model.

Keywords: Fiber Bragg grating sensor, strain sensor, enhanced strain sensitivity, dam model

1. GENERAL INSTRUCTIONS

The seismic safety of existing concrete dams is a major concern due to the catastrophic consequences of a sudden release of the reservoir if the dam fails under strong ground motions. The state of knowledge in structural dynamics and seismicity is continuously progressing such that the seismic safety of concrete dams should be periodically evaluated considering the latest assessment of their strengths and the ground motion intensity to which they might be subjected (Tinawi etal, 2000). Although substantial progress has been achieved in mathematical modeling for dam safety in the area of dam engineering (Fenyes, 1992) (Bruhwiler, 1990), few of the various models have been verified and are still unable to precisely evaluate the seismic safety of real dams in the critical state (Zhou, 2000). Dam model testing on shake tables has the potential of being used for analysis verification purposes and seismic safety evaluation subjected by different intensities of ground motion.

In addition to theoretical analysis, there are a number of experimental shake table tests that were conducted on small scale models to predict the seismic response of gravity dams (Donlon, 1991) (Lin, 1993) (Mir, 1996). To achieve experiments aimed toward testing the cracking response and failure modes of dam, the models were built from special material with low tensile and compressive strength to conform to the laws of similitude. Accurate measurement of strain variation and effective prediction of failure inside the model has been a major objective of strain sensors for dam model tests.

Electrical strain gauge is a custom sensor applied widely in strain measurement with the advantages of easy disposition, cheap price and tolerable measurement accuracy. However, due to the electromagnetic interference of the shake table, the stability of the electrical strain gauge cannot satisfy the demand of long-range strain monitoring (Ren, 2006). Furthermore, it is difficult to bond the electrical strain gauge to the surface of dam model due to the low Young's modulus of the model material. FBG strain sensors, which have superior immunity to electromagnetic interference, high

accuracy, and especially embedability in the structure (Kersey, 1997) (Li, 2004), are ideal for measurement applications in the simulated seismic tests of dam models.

However, an FBG sensor made with a bare fiber is fragile in the direction of shear force and easily damaged when handled improperly during and after fabrication. Some protective packaging of FBG, such as backing patch (Betz, 2006) and embedded packaging (Zhao, 2003), have been proposed to prevent the damage of the bare FBG. The operation principle of FBG strain sensors with packaging of backing patch depends on the bare FBG bonding to the surface of a polymer or metal patch with pre-groove using the epoxy glue. The embedded packaging is such that the bare FBG is embedded in a metal tube with epoxy resin or the polymer material (Moyoa, 2005) directly. Though these packaging techniques have advantages of simple structure, easy packaging and convenient installation, the strain transferring loss, which decreases the strain sensitivity of FBG sensor, inevitably exists between the packaging and measurand material, especially in the case of low Young's modulus of the measurand material.

In this paper, a FBG strain sensor with enhanced strain sensitivity and packaged by two gripper tubes is presented and applied in the seismic tests of a small scale dam model. The objectives of this study are the following:

To present the sensor design theory, including an introduction of the sensing principle of the FBG packaging mechanism. A derivation of the theoretical strain sensitivity will be presented to study the characteristics of the presented FBG strain sensor, including comparisons between calibrated strain sensitivity of sensor with theoretical results.

To investigate the applicability of the FBG strain sensors in seismic tests of a dam model by conducting a comparison between the test measurements of FBG sensors and analytical predictions, to monitor the failure progress and predict the cracking inside the dam model considering the maximum tensile strain variation, the residual strain variation and the strain course during test of each FBG sensor.

2. SENSOR DESIGN THEORY

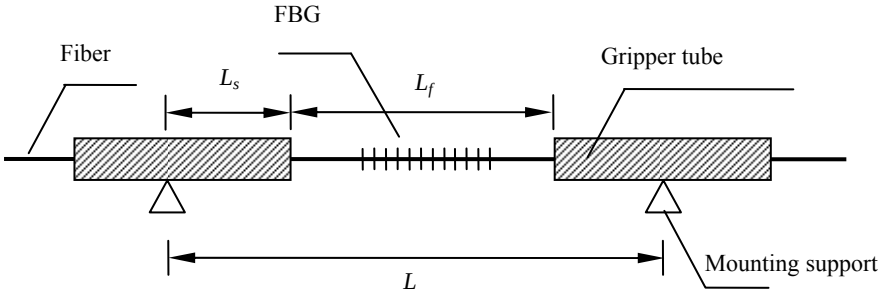

Figure 1 The schematic diagram of FBG strain sensor packaged by two gripper tubes

The schematic diagram of a FBG strain sensor is presented in Figure 1. The strain sensor consists of a fiber Bragg grating, two gripper tubes and two mounting supports. The fiber in both sides of a FBG is packaged with epoxy resin in the two gripper tubes, which are installed on the mounting supports by adhesive or solder. Since the FBG area is not in contact with epoxy resin, the FBG strain sensor eliminates the multi-peaks of reflective light from FBG induced by the non-uniform bonding distribution of epoxy resin. When the thickness of the glue is less than the diameter of an optical fiber, the stress transferring loss between epoxy resin and fiber can be neglected, as it has been discussed in detail (Yung, 2005), and the deformation of gripper tube and FBG are written as

$$\Delta L_s = \frac{P_s L_s}{E_s A_s} \tag{2.1}$$

$$\Delta L_f = \frac{P_f L_f}{E_f A_f}, \tag{2.2}$$

where E_s, E_f, A_s and A_f are Young's modulus and sectional area of gripper tube and fiber, respectively, the distance between two mounting supports and the length of fiber are L and L_f, respectively, and P_s *and* P_f are the internal tension forces in the fiber and the gripper tubes, respectively. Since the value of the tension forces are constant throughout the sensor structure, P_s equals to P_f. Therefore, the strain ratio between gripper tube and fiber can be expressed as

$$\frac{\varepsilon_s}{\varepsilon_f} = \frac{\Delta L_s / L_s}{\Delta L_f / L_f} = \frac{E_f A_f}{E_s A_s}. \tag{2.3}$$

Table 1 presents the mechanical properties of the FBG strain sensor. The strain ratio is obtained by substituting the parameter values into (2.3) as

$$\frac{\varepsilon_s}{\varepsilon_f} = 0.0084. \tag{2.4}$$

Table 2.1 Mechanical properties of the optical fiber

Component	Young's modulus[Pa]	Diameter[mm]
Fiber core (E_f)	72×10^9	0.125
Gripper tube (E_s)	210×10^9	0.8

It is drawn from (2.4) that the strain of the gripper tube can be neglected in contrast with the strain of fiber in the above sensor construction. The fiber between the two gripper tubes bears nearly the whole deformation between the two mounting supports. For a FBG with central wavelength of 1550nm, the relation between the shift of the central wavelength of FBG and the strain of the sensor can be written as

$$\varepsilon = \frac{L_f}{L}\varepsilon_f = \frac{L_f \Delta\lambda_{FBG}}{1.2L}. \tag{2.5}$$

The strain sensitivity of sensor is decided by the ratio of the distance between the two mounting supports L and the length of the fiber between the two gripper tubes L_f, as shown in (2.5). For the case that L is bigger than L_f, the sensor has a mechanical structure of strain sensitivity amplification. A suitable strain sensitivity of FBG strain sensor can be obtained by adjusting the ratio between L_f and L.

3. RESULTS OF SENSOR CALIBRATION AND RELIABILITY TESTS

3.1. Sensor and experimental setup

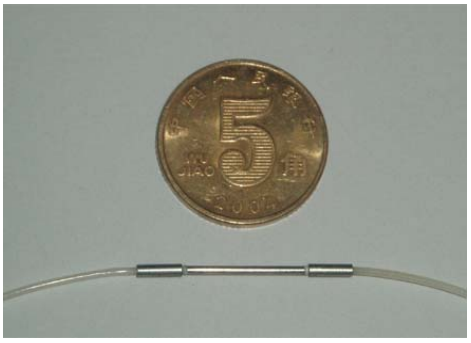

Figure 2 The picture of gripper packaged FBG strain sensor

The FBGs used in this work were inscribed in Ge-doped photosensitive optical fiber using the phase mask technique. The gratings were annealed for more than 7h at 200℃ to stabilize the performance of the FBG. The picture of gripper packaged FBG strain sensor is presented in Figure 2. The distance

between two mounting supports L and the length of fiber between the two gripper tubes L_f of the FBG strain sensor were 15mm and 9mm respectively. The strain amplification factor was thus 15/9. It is derived from (2.5) that the calculated strain sensitivity of FBG strain sensor was 0.5με/pm.
To characterize the working performance of the FBG strain sensor in dissimilar host material with different Young's modulus, a series of calibration tests of FBG strain sensor were conducted on the steel and plastic plates, of which the Young's modulus were 2.1×10^5 MPa and 3×10^3 MPa, respectively. A FBG strain sensor and a strain gage were mounted directly on the plates within the cyanoacrylate adhesive. Then, the tensile tests in the steel and plastic plates were carried out in the material testing system.

3.2. Results of sensor calibration tests

The steel and plastic plates were loaded continuously from 0με to 1000με and 700με, respectively. In the linear elasticity range of steel and plastic, the strain value was considered identical between FBG strain sensor and strain gage. To ensure repeatability and better averaging of the results, all measurements were taken several times.

The results of the calibration tests obtained are plotted in Figure 3, showing the relationship between the Bragg wavelength shift of the FBG strain sensor and the strain value of strain gage. Excellent agreement between strain gages and the FBG strain sensor was observed at the load level and the coefficient of linear association is more than 0.9999. The experimental strain sensitivities of FBG strain sensor in steel and plastic plates are 0.501με/pm and 0.487με/pm, respectively, as shown in Figure 3. The experimental values agree well with the calculated strain sensitivity of the FBG sensor. In addition, the strain transferring loss in the plastic plate is very small and can be neglected. The results prove that the FBG strain sensor works well on host materials with low Young's modulus, such as plastic.

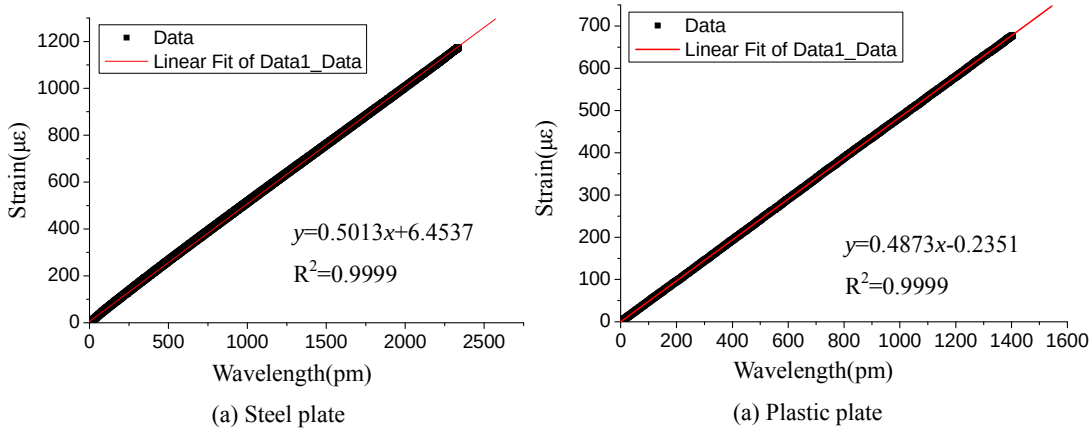

(a) Steel plate (a) Plastic plate

Figure 3. Results of FBG strain sensor calibration tests

3.3. Sensor reliability tests

Reliability is an important aspect of any sensor, especially in terms of long term monitoring of civil structures, such as bridges and dams with 50 to 100 years' service life. In order to investigate the reliability of the FBG strain sensor, a uniform-strength beam was used as a test structure with continuous deformation loaded by a material test machine (MTS810), which applies axial sinusoid force from 0.1KN to 6.1KN at a constant speed, as shown in Figure 4.

Since the strain on both surfaces of the uniform-strength beam has equal magnitude and contrary sign, two FBG strain sensors (Sensor A and Sensor B) were mounted on both surfaces of the uniform-strength beam within the cyanoacrylate adhesive to investigate the reliability of sensors under tensile and compressive load. Sensor A and Sensor B were compared with each other. The central wavelength of FBG sensors were recorded during 1200 load cycles.

The partial data of loading-unloading cycles for FBG strain sensors are shown in the Figure 5. To eliminate the effects due to temperature variation during the reliability tests, the difference between the maximum and minimum wavelengths at intervals of 100 load cycles for each sensor were calculated and are shown in Figure 6. There are ten such wavelength variations for total 1200 load cycles. The differences for Sensor A are outlined with blue rhombuses in the top of Figure 6, whereas Sensor B's are outlined with pink squares in the bottom of Figure 6. Furthermore, both tensile and compressive strains can be easily measured without a post-tensioned FBG configuration. The results demonstrate that the behavior of FBG strain sensors is steady and repeatable in the reliability test, as shown in Figure 6.

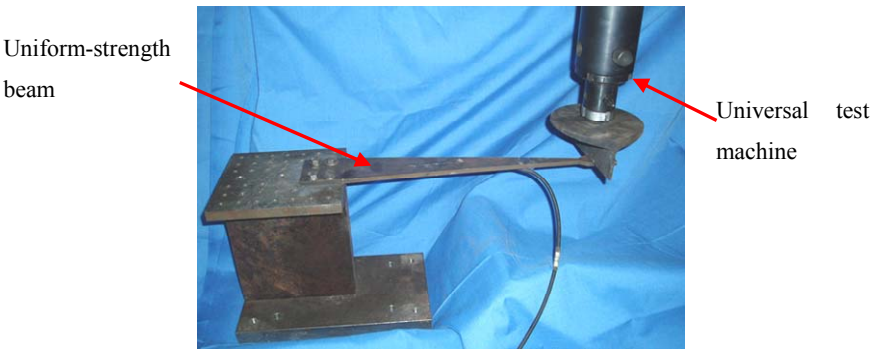

Figure 4. Reliability test set-up of FBG strain sensor

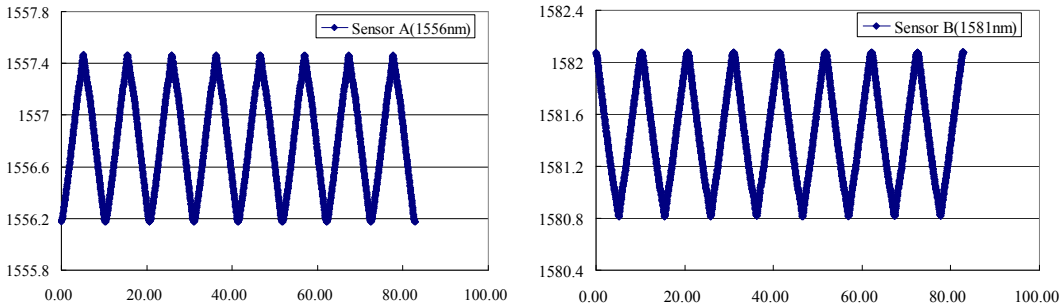

Fig. 5. The data of loading and unloading circles saved by Sensor A and Sensor B.

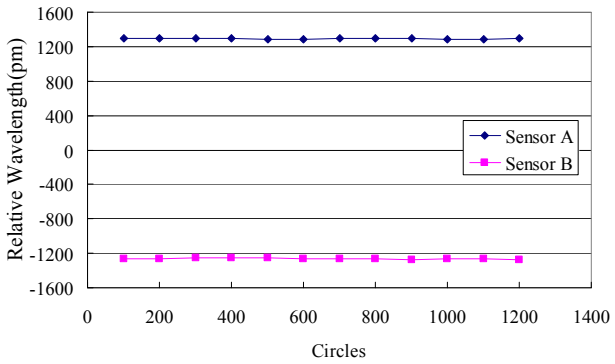

Figure 6. Reliability investigation results of FBG strain sensors

4. APPLICATION OF FBG STRAIN SENSORS IN THE SMALL SCALE DAM MODEL

4.1. Dam model and instrumentation setup

A configuration similar to that of the existing concrete gravity arch dam located on Dadu River near Ya'an, Sichuan province, was selected for the purpose of modeling. This concrete dam's configuration is a hyperbolic arch. For the seismic intensity of the area, the dam has the magnitude of eighth and the tallest monolith exceeds 200m. In addition to theoretical analysis, it is necessary to conduct dam model seismic simulation tests to evaluate the seismic resistant performance of the dam. A series of dam model tests on the shaking table were conducted to study the dynamic response and the failure

state of the dam model under different magnitude of simulated seismic wave.

The unreinforced concrete dam model is built to scale 1:273 according to the dimension and maximum load of the shake table. The material of the model, which consists of cement, river sand, heavy quartz sand, heavy quartz powder, iron powder and water, has low tensile and compressive strengths of 0.0175MPa and 0.45MPa, respectively. Because the stress-strain curve, the accumulated failure curve and the fracture characteristic of model material are similar to those of mass concrete, it is suitable to investigate the characteristics of concrete dam in the elastic, elastic-plastic and fracture ranges.

There were ten gripper-tube packaged FBG strain sensors embedded in the crest of the dam model with the depth of 10mm for the dynamic strain monitoring. The arrangement of sensors is shown in Figure 7 and Table 2 lists the specification of the FBG sensors.

A tunable Fabry–Perot filter system from Micron Optics Inc. was used as the readout unit for the FBG strain sensors. This interrogation technique allows the simultaneous detection of several sensors in series; their total number depends on the expected dynamic range of strain. The system has a temperature-stabilized fixed Fabry–Perot multiwavelength reference to achieve stability and accuracy of 2 pm at one measurement.

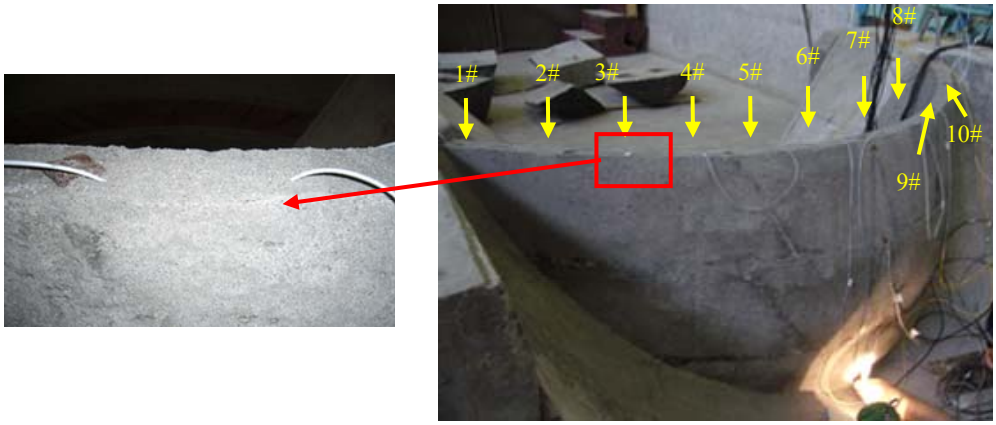

Figure 7. Positions of FBG sensors and the partial enlarged drawing after installation

Table 2 The central wavelength of FBG sensors

Semsor Number	1#FBG	2# FBG	3# FBG	4# FBG	5# FBG
Central wavelength(nm)	1545.56	1548.53	1550.95	1548.93	1550.90
Sensor Number	6# FBG	7# FBG	8# FBG	9# FBG	10# FBG
Central wavelength(nm)	1544.88	1552.75	1544.77	1548.19	1553.12

4.2. Simulated seismic tests, Results, and Analysis

The dam model was subjected to ground seismic wave with incremental magnitude to observe its cracking response. The ground seismic wave is derived from the seismic wave of the area of Dagangshan dam with 2% exceeded probability in 50th years. Table 3 and Figure 8 presents the observed cracking record due to the increasing magnitude of ground seismic waves.

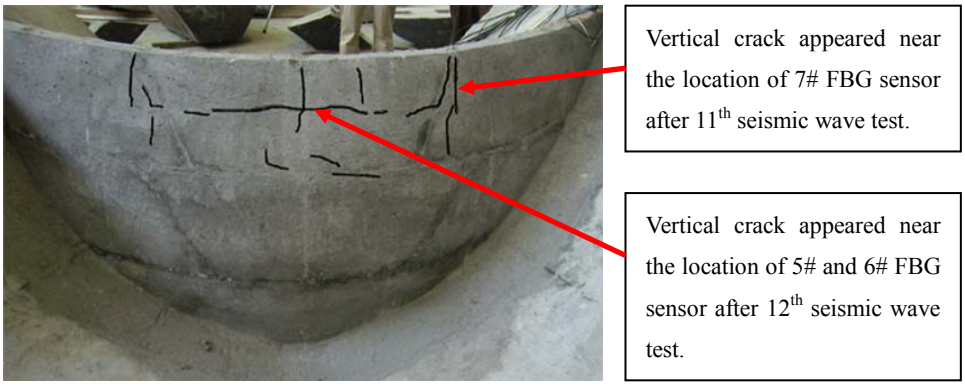

Figure 8. Observed cracking of dam model on upstream face

Table 3 The observed cracking record

Magnitude of seismic wave	Observed cracking record	Input maximum acceleration(Gal)
1^{st}~5^{th}	No crack	0.065, 0.134, 0.181, 0.242, 0.280 respectively
6^{th}~10^{th}	No crack	0.333, 0.373, 0.431, 0.465, 0.507 respectively
11^{th}	Vertical crack appeared near the location of 4# and 7# FBG sensor	0.581
12^{th}	Vertical crack appeared near the location of 5# and 6# FBG sensor	0.696

To evaluate the performance of the dam model setup, a comparison is made between the test measurements and analytical predictions. The results of finite element analysis and the test measurement of the model were obtained for the input ground seismic wave with 3^{rd} magnitude, as shown in Figure 9. It is shown that the dam crest strain response to a seismic wave is maximal in the middle of the crest and gradually reduces toward both ends. The maximum strain distribution of the crest of dam model measured by FBG strain sensors and calculated by finite element analysis are in good agreement. The small difference between measurement and finite element analysis results is induced by non-uniformity of the model material and local failure during the demolding procedure.

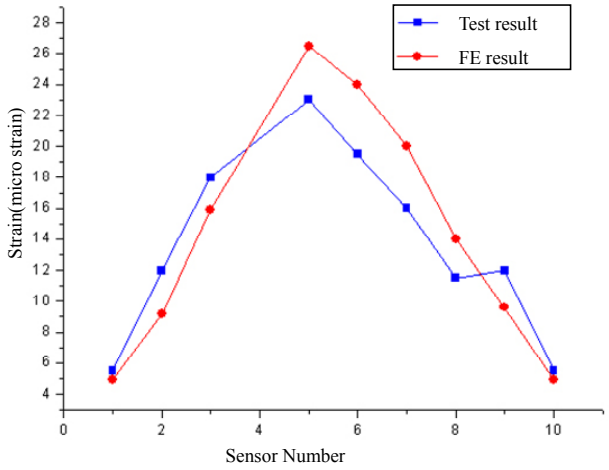

Figure 9. Comparison of maximum strain between measured values and theoretical results induced by seismic wave with 3^{rd} magnitude

4.3. Failure identification of dam model by FBG strain sensors

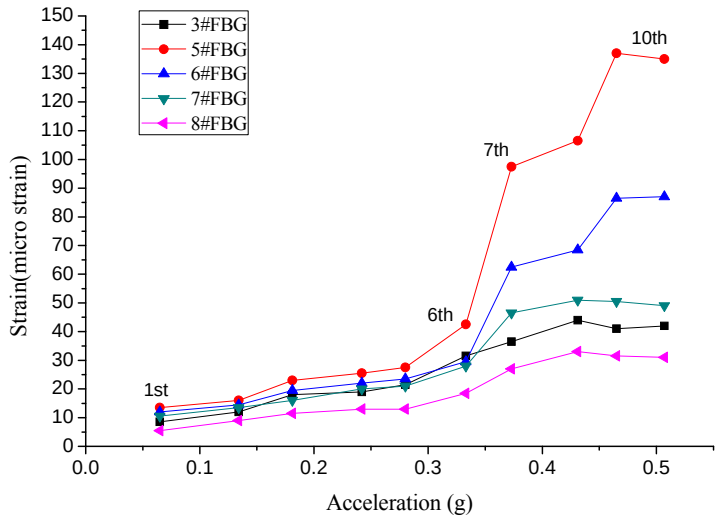

Figure 10. Maximum tensile strain variation of FBG strain sensors during different seismic waves with incremental magnitude

Because the tensile strength of the model material is far less than the comressive strength, the failure in the dam model, which is mainly caused by the effect of excessive tensile strength, can be identified by monitoring the maximum tensile strain variation. Figure 10 shows the maximum tensile strain variation of FBG strain sensors during different seismic waves with incremental magnitude. The maximum tensile strain recorded by FBG strain sensor was linear to the input maximum acceleration from the 1st to the 6th seismic test. The dam model behavior remained elastic until the 7th seismic test, when the response of the maximum tensile strain became nonlinear for redistribution of the stress field induced by failure in the model crest, as it is recorded by 5#, 6# and 7# FBG sensor. As expected, the maximum tensile strains recorded 5# and 6# FBG sensors increased apparently, which are in good agreement with the theoretical results.

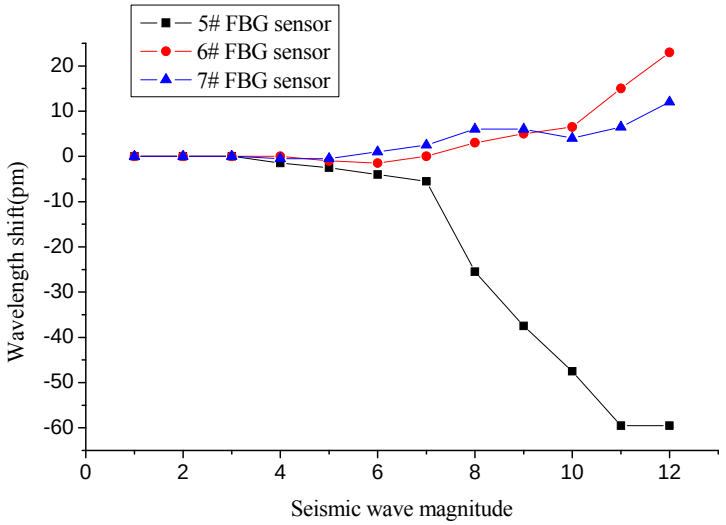

Figure 11. The residual strain variation of FBG sensors during different seismic waves with incremental magnitude

Supposing the strain of the FBG sensors before the model tests was the initial strain of each sensor, the difference between the strain after every seismic test and the initial strain is defined as residual strain of each sensor, which reflects the state of the stress field redistribution inside the model dam. The variation of residual strain recorded by 5#, 6# and 7# FBG sensor is shown in Figure 11. The residual strains of these sensors are approximately zero for the elastic state of the dam model before the 7th seismic test. There is a remarkable variation of residual strain monitored recorded by 5#, 6# and 7# FBG sensor after the 7th seismic test, which can be explained if some cracking occurred near the

locations of these FBG sensors and caused irreversible deformation of the dam model.
Figure 12 shows the strain course of 5# FBG sensor during the 6th and the 7th seismic test. Figure 12(a) shows that the central wavelength of the FBG sensor is approximately a constant before and after the 6th seismic test due to the elastic state of the dam model. With increasing input acceleration of the seismic wave, the central wavelength of the FBG sensor generates a remarkable alteration before and after the 7th seismic test, as shown in Figure 9(b). A result can be drawn that some cracking was produced near the location corresponding to the 5# FBG sensor during the 7th seismic test.

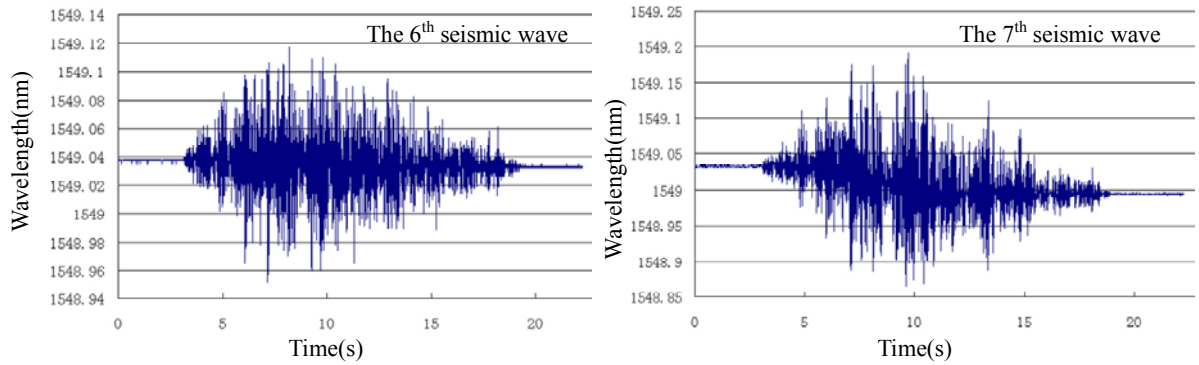

Figure 12. The strain course of 5# FBG sensor during the 6th and the 7th magnitude of seimic tests

5. CONCLUSION

A new configuration for a FBG strain sensor with the function of controlled enhanced strain sensitivity was characterized, calibrated and applied in the small scale model testing of a concrete gravity dam. The calibration experimental results demonstrate that the experimental strain sensitivity of the sensor agrees well with the calculated result derived by analysis of the sensor's packaging mechanism. It has been found that this FBG strain sensor works well on materials with low Young's modulus, such as plastic, and its repeatability was demonstrated in the reliability test.

Some FBG strain sensors have been embedded in the crest of a dam model for failure progress monitoring and cracking identification during simulated seismic wave tests actuated by shake table. A good agreement was obtained between the maximum strain distribution of the crest of the dam model measured by FBG strain sensors and calculated by FE analysis. The results show that the failure and cracking of the dam model can be identified by analyzing the maximum tensile strain variation, the residual strain variation and the strain course during test of each FBG sensor. Results of the dam model tests prove that this FBG strain sensor has the advantages of small size, high precision and embedability, demonstrate promising potentials in the cracking and failure monitoring and identification of dam model.

ACKNOWLEDGEMENTS
This work has been supported by the Science Fund for Creative Research Groups of the National Natural Science Foundation of China (Grant No. 51121005), the Natural Science Foundation of China (Grant No. 51108059, No.50978045), and the Key Laboratory Foundation of Liaoning Province (Grant JG-200909). These grants are greatly appreciated.

REFERENCES

Bruhwiler, E., and Wittmann, F. H. (1990). Failure of dam concrete subjected to seismic loading conditions. *Engrg. Fracture Mech.* 35, 565–571.
D. C. Betz, G. Thursby, B. Culshaw. (2006). Advanced layout of a fiber Bragg grating strain gauge rosette, *Journal of lightwave technology* 24:2, 1019-1026.
Donlon, N. W. P., and Hall, J. F. (1991). Shaking table study of concrete gravity dam monoliths. Earthquake *Engrg. and Struct. Dyn*. 20, 769–786.

Fenves, G. L., Mojtahedi, S., and Reimer, R. B. (1992). Effect of contraction joints on earthquake response of arch dam. *J. Struct. Engrg.* ASCE, 118:4, 1039–1055.

Kersey AD, Michael AD, Heather JP, Michel L, Koo KP, Askins CG, Putnam MA, and Friebele EJ. (1997). Fiber grating sensors. *Journal of lightwave technology* 15:8, 1442-1463.

Li Hong-nan, Li Dong-sheng and Song Gangbing. (2004). Recent applications of fiber optic sensors to health monitoring in civil engineering. *Engineering Structures*. 26:11, 1647-1657.

Lin, G., Zhou, J., and Fen, C. Y. (1993). "Dynamic model rupture test and safety evaluation of concrete gravity dams." *Dam Engrg.* 3, 144–173.

L. Ren, J. Zhou, L. Sun, and D. Li. (2006) "Application of tube-packaged FBG strain sensor in vibration experiment of submarine pipeline model," *China Ocean Eng*. 20:1, 155–164.

Mir, R. A., and Taylor, C. A. (1996). An investigation into the base sliding response of rigid concrete gravity dams to dynamic loading. *Earthquake Engrg. and Struct. Dyn.* 25, 79–98.

P. Moyoa, J.M.W. Brownjohn, R. Suresh, S.C. Tjin. (2005) Development of fiber Bragg grating sensors for monitoring civil infrastructure, *Engineering Structures*, 27, 1828–1834.

R Tinawi, P Leger, M Leclerc, G Cipolla. (2000). Seismic Safety of Gravity Dams: From Shake Table Experiments to Numerical Analyses. *J. Struct. Engrg.* 126, 518-529.

XF. Zhao, SZ. Tian, Z. Zhou, LB. Wan, JP. Ou. 2003. Experimental Study on Strain Monitoring of Concrete Using a Steel Slice Packaged Fiber Grating. *Journal of Optoelectronics.laser* 14:2, 171-174.

Yung Bin Lin, Kuo Chun Chang, Jenn Chuan Chern and Lon A. Wang. (2005) Packaging Methods of Fiber-Bragg Grating Sensors in Civil Structure Applications, *IEEE SENSORS JOURNAL* 5, 419-424.

Zhou J, Lin G, Zhu T, et al. (2000). Experimental investigations into seismic failure of high arch dams. *Journal of Structural Engineering*, 126:8, 926-935.